

Statistical Analysis of In-Situ End-Point Detection in Copper Chemical-Mechanical Polishing

Kyungyoon Noh and Elizabeth Lyon

Abstract—This paper presents statistical techniques for analysis in-situ end-point data in Cu CMP. An optical reflectance sensor is employed on a rotary polishing tool to measure the surface reflectance of patterned Cu wafers. Statistical models are developed to determine the surface condition based on the characteristics of the sample reflectance data. A nested variance model is proposed to decouple the variance components of within-wafer and within-die non-uniformity. This information may be employed to control the process parameters to improve the material removal rate and the within-wafer uniformity. Algorithms based on the changes in mean, variance, range and distribution of the surface reflectance are examined for their effectiveness in process monitoring and end-point detection.

Index Terms—Chemical-Mechanical Polishing (CMP), End-Point Detection (EDP) and Statistical Process Control (SPC).

I. INTRODUCTION

Continuing advances in ultra-large-scale integration (ULSI) technology require the fabrication of submicron-size features of higher resolution, denser packing and multi-layer interconnects. In the past decade, chemical-mechanical polishing (CMP) has been successfully employed to smooth surface topography of inter-level dielectrics (ILD) and multi-level Cu damascene structures. Over the past several years, copper has emerged as the optimal interconnect material because of its low electrical resistivity and resistance to electromigration. Patterned Cu lines are produced by a damascene scheme, comprising oxide trench patterning and Cu deposition, followed by CMP. The current success in producing high resolution interconnects is due to the excellent local and global planarization capabilities of the Cu CMP process.

The main challenge for most of CMP applications is to control non-uniformities of the surface topography to meet the more stringent wafer- and die-level planarity requirements for various substrate materials. These non-uniformities will vary the cycle time, or the end-point, of the Cu CMP and affect the process yield. In order to reduce the variance of uniformity, it is necessary to integrate an *in situ* sensing and end-point detection

technique with the process optimization schemes to improve process performance.

The ideal wafer-level end-point for Cu CMP process may be defined as the time when the excess Cu and barrier layers are fully cleared on all dies of a wafer. Due to polishing nonuniformity, however, all the dies on a wafer generally will not reach the end-point at the same moment. Some of the dies may be overpolished. Thus the end-point of CMP can be a representation of the optimal polishing time when the number of out-of-specification dies reaches a minimum. However, the remaining Cu thickness in each die area is difficult to measure in real-time due to its dynamic environments.

Among the current end-point detection techniques, the optical sensing techniques of interferometry and reflectance measurement provide the localized means for detecting the end-point. Specially, the reflectance measurement is ideal for detecting the surface topography and the metal area fraction on the surface. Most of end-point methods are limited in practical applications by lack of reliability and high noise-to-signal ratio. These techniques focus mainly on average information over a relative large area, usually wafer-level [2, 6, 8, 10].

Several issues must be resolved to fully utilize the reflectance measurement technique. The signal from the sensor cannot be unambiguously interpreted because it contains both systematic and random attributes of the surface condition of the polished surface and the polishing environment. The reflectance varies across the wafer due to the nonuniform pattern layout and within-wafer nonuniform polishing. These effects must be decoupled to gain information for polishing uniformity control. In addition to the interpretation of the signal, the sensor kinematics must be studied to map the data onto the wafer surface to gain both wafer- and die-level information. An adequate spatial resolution for indicating local conditions can be achieved through sensor trajectory design. Such information will increase the confidence level of interference about the wafer surface condition, and will lead to a more accurate and repeatable decision-making for the end-point detection.

This research employs the in-situ reflectance measurement technique on patterned Cu wafers in Cu CMP. A statistical model is developed to decouple the variation of the surface reflectance and to estimate the variance components contributed by nonuniform polishing due to pattern variation and within-wafer nonuniform polishing. Algorithms for utilizing those two techniques in process end-point monitoring and control are also discussed.

Elizabeth Lyon is a graduate student in the Department of Materials Science and Engineering, Massachusetts Institute of Technology, MA 02139 USA.

Kyungyoon Noh is a graduate student in the Department of Mechanical Engineering, Massachusetts Institute of Technology, MA 02139 USA

II. THEORY

A. Reflectance in a Cu damascene structure

In the Cu damascene structure, the number of possible modes for the scattering field is limited by the surface condition. If the wavelength of the incident light is close to the waviness of the pattern, there will be only one mode and the surface will reflect secularly regardless of the surface topography. For the sub-micron Cu patterns employed in the current design, the reflectance measured at the onset of the process end-point by a light source with comparable or larger wavelength will essentially indicate the Cu area fraction only. The slight surface topography due to overpolishing and dishing will not significantly affect the reflectance. The surface reflectance R , proportional to the square of the reflection coefficient, of the composite surface at the onset of end-point therefore can be written as:

$$R = A_f R_{Cu} + (1 - A_f) R_{Oxide} \quad (1)$$

where, A_f is the area fraction of Cu interconnects, and R_{Cu} and R_{oxide} the reflectances of Cu and TEOS, respectively, in specular reflection.

B. Sensor Kinematics

The sensor loci on the rotating wafer surface can be determined by the relative velocity of the sensor to the wafer and the initial position of the sensor, as shown in Fig. 1. The relative velocity of the sensor on the rotating wafer can be obtained by two steps: find the relative velocity of the sensor to the stationary X, Y coordinates fixed at the center of the wafer and then perform a coordinate transformation with respect to the wafer rotation. The velocity components for the sensor, $v_{X,s}$ and $v_{Y,s}$, and the wafer, $v_{X,w}$ and $v_{Y,w}$, in X, Y coordinates can be expressed as:

$$\begin{aligned} v_{X,s} &= -r_s \omega_p \sin(\omega_p t + \theta_0) - \dot{r}_{cc} \quad (2) \\ v_{Y,s} &= r_s \omega_p \cos(\omega_p t + \theta_0) \\ v_{X,w} &= -r_s \omega_w \sin \theta \\ v_{Y,w} &= \omega_w (r_s \cos \theta - r_{cc}) \end{aligned}$$

where, r_s is the offset of the sensor from the center of the platen, r_{cc} the offset of the centers of the wafer and the platen, ω_w and ω_p are the angular velocity of the wafer and the platen, and θ the angle of the sensor with respect to the X coordinate.

When the angular velocities of the wafer and the platen are the same, the sensor enters the wafer/pad interface at the same point on the periphery of the wafer. It always produces the same locus on the wafer surface. But in practice, the angular velocity of the wafer must be slightly offset from the platen so that the sensor can scan over the entire wafer surface in different radial directions as shown in Fig. 2. As illustrated, the sampling density will be much higher at the center of the wafer, and lower at the edge where more dies are located. The lower sampling density on the edge dies might result in bias inference for the overall surface condition. Therefore, the way to design sensor loci to sample enough data on a desired surface area should be discussed.

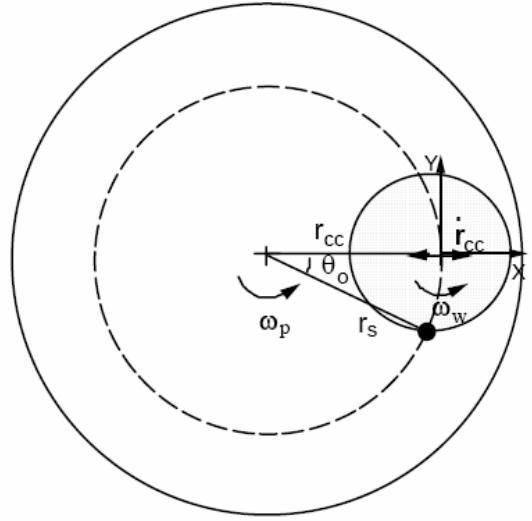


Fig. 1. Schematics of sensor kinematics

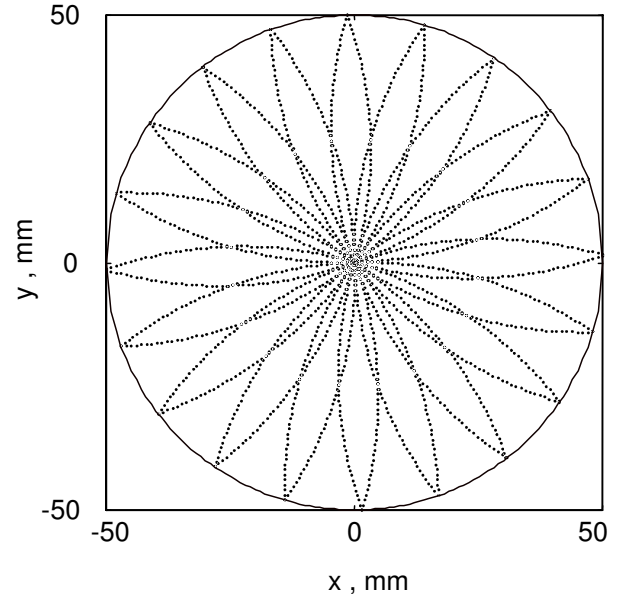


Fig. 2. The simulated locus for the reflectance sensor across the wafer at the condition $\omega_w = 1.05\omega_p$ and $r_s = r_{cc}$.

C. Sampling Strategy

Three levels, wafer-, die- and device- or subdie-level, of information can be obtained from the reflectance measurements. The spot size of the sensor is chosen so that it is comparable to or smaller than the subdie area but still much larger than the dimensions of interconnects. Therefore, an individual measurement represents the reflectance on the specific device or pattern area on the wafer, from which the surface topography and Cu area fraction can be inferred. It is difficult to map the measurement results onto the exact location of a particular device or pattern because of wafer slippage inside the carrier. The individual datum can only be mapped onto the surface within a grossly defined area. Similarly, the die-level information may be obtained along a specific segments corresponding to the die location on the loci. Moreover, wafer-level informa-

tion can be retrieved either from a single or multiple scans across the wafers. In end-point detection, it is preferable to take samples from multiple loci so that the surface condition over a specific region or the entire wafer surface can be determined from the pooled dataset. The more loci employed, the larger, more uniform samples can be taken. Therefore, a higher level of inference can be achieved. However, there is a possibility that the surface condition may change significantly during the long sampling period needed for multiple scans. This may affect the reliability of the inference and will delay decision making and feedback control. The moving average method is used to estimate the average reflectance on the surface to eliminate this problem. The sensor scans the wafer surface once per platen revolution. If the reflectance sampled at the j -th point along the locus at the i -th time period, each time period is equal to the duration for one revolution of the platen, denoted as x_{ij} . If total n points are taken along each locus, the mean reflectance along the locus at the i -th period, \bar{x}_i , is:

$$\bar{x}_i = \frac{1}{n} \sum_{j=1}^n x_{ij} \quad (3)$$

Suppose the number of loci to cover the entire wafer surface or a area of interest is w , the moving average of the sampling reflectance at the i -th period, M_i , is defined as:

$$M_i = \frac{\bar{x}_i + \bar{x}_{i-1} + \dots + \bar{x}_{i-w+1}}{w} \quad (4)$$

That is, at the i -th time period, the observations from the newest one scan and the previous $(w-1)$ scans are employed to estimate the mean reflectance of the entire wafer or the surface of interest. Thus, the surface condition as inferred from the reflectance measurements can be updated every scan. The moving average can capture the change of surface reflectance due to both the change of surface topography and the change of Cu area fraction within a short period, in this case in less than one second. However, it may still smooth over the rapid change due to the partial oxide exposure on small portions of the wafer surface near the onset of end-point by averaging the current data with the previous data.

The total variance of the surface reflectance at i -th time period, S_i^2 , can be estimated based on the same pooled dataset employed in the moving average:

$$S_i^2 = \frac{\sum_{i-w+1}^i \sum_{j=1}^n (x_{ij} - M_i)^2}{N - 1} \quad (5)$$

where, N is the total number of samples in the moving average subset ($N = wn$). The total variance is calculated based on the deviation of the reflectance at each sampling point relative to the total estimated mean of the surface of interest, as estimated by the moving average. In addition to the total variance, the variance along each locus, the range of data, and their maximum and minimum must be tracked to identify the rapid change of surface reflectance at the moment when the barrier or oxide layer is exposed. The variance can determine the percent

of overpolished area on the wafer surface at the end of the process. Additionally, the distribution of the data can determine the regime of polishing.

D. Spatial Nonuniformity

In this research, we will measure the spatial variation using a metric which normalizes the variation by the mean. The fundamental ratio that we will consider is:

$$N_i \equiv \left(\frac{\sigma}{\mu} \right)_i = \frac{S_i}{M_i} \quad (6)$$

where σ is the observed standard deviation and μ is the observed mean of one reflectance path. This ratio is commonly used as a expression of wafer-level non-uniformity [3, 5].

E. Variance Components of the Surface Reflectance

The surface reflectance of a patterned wafer varies with the surface roughness, pattern topography and area fraction, and optical properties of the coatings. Due to the within-wafer nonuniform material removal, the surface topography and the remaining fraction of Cu during polishing may vary among different dies across the wafer. The within-wafer nonuniform polishing usually results from certain systematic sources, such as nonuniform velocity distribution, pressure distribution, interfacial temperature distribution, slurry flow, and contact conditions. Their effect on polishing always follows a systematic pattern which tends to be repeatable between wafers of the same lot. The wafer-level nonuniformity affects the pattern evolution on the same die with a similar trend. The relative rates of material removal between different patterns on a die will remain similar to another die at different location because the factors that affect wafer-level nonuniformity will have less interaction with the die- or device-level polishing behavior. For instance, die-level polishing is mostly affected by the pattern geometry, such as linewidth and area fraction. Therefore, the variation of reflectance measurements on a die tends to follow the same distribution and is nested within the die. Based on this assumption, a two-level nesting variance structure is employed to decompose the effects of within-wafer and die-level non-uniform polishing [5]. Assuming that the reflectance at each level is normally distributed, the reflectance at location j of die i on the wafer, R_{ij} , can be written as:

$$R_{ij} = \mu + W_i + D_{j(i)} \quad (7)$$

where, μ is the average reflectance within the wafer from multiple loci, W_i the die-to die (or within-wafer) effect on die i , and $D_{j(i)}$ the within-die effect at location j on die i . The total, within-wafer and within-die variances of surface reflectance are expressed as σ_T^2 , σ_W^2 , σ_D^2 respectively. Additionally, the within-die effect, $D_{j(i)}$, is assumed to be normal and the two-level variance components are assumed to be independent to each other. Therefore, the total variance of reflectance, σ_T^2 , can be written as:

$$\sigma_T^2 = \sigma_W^2 + \sigma_D^2 \quad (8)$$

If the sampling plan is balanced, i.e., same number of measurements are taken at each level on each sample, the variances of each level can be estimated by the following analysis. The variance component for within-die effect, S_D^2 , can be estimated by:

$$S_D^2 = \frac{1}{m} \sum_{i=1}^m \sum_{j=1}^n \frac{(x_{ij} - \bar{x}_i)^2}{n-1} \quad (9)$$

Where m is the number of dies sampled, n the sample size at each die, \bar{x}_i the mean of reflectance at die i . The within-wafer variance σ_W^2 can be obtained by using the relation between the variance of die means, $\sigma_{\bar{W}}^2$, which can be represented as:

$$\sigma_{\bar{W}}^2 = \sigma_W^2 + \sigma_D^2 / n \quad (10)$$

The variance of die means $\sigma_{\bar{W}}^2$ can be estimated by $S_{\bar{W}}^2$:

$$S_{\bar{W}}^2 = \sum_{i=1}^m \frac{(\bar{x}_i - \hat{x})^2}{m-1} \quad (11)$$

where \hat{x} is the grand mean of the measurements, the moving average of multiple scans over a given span in this case.

Finally, we can use a F-ratio analysis between wafer-level variance and die-level variance to as one of reference to check end-point [3].

$$F = \frac{S_{\bar{W}}^2}{S_D^2} \quad (12)$$

III. EXPERIMENTS

An optical sensor unit comprising of light-emitting diodes (LEDs), bundled glass fibers for light transmission and receiving, and an amplifier detected the conditions of the wafer surface based on surface reflectance. Table 1 lists the specifications of the sensor.

TABLE 1
SPECIFICATIONS OF THE REFLECTANCE SENSOR

Item	Specification
Light Source	High Intensity LED
Wavelength (nm)	780-990 ($\mu=880$, $\sigma=50$)
Spot Diameter (mm)	1.6
Light Beam Spread ($^\circ$)	30
Operation Distance (mm)	0-6.35
Stability (%)	<0.1% full scale
Frequency Response (kHz)	< 20

The sensor unit was installed on the platen base with the tip embedded inside a holder through the platen. A translucent plastic window allowed the sensor view the wafer surface through the polyurethane polishing pad stacked on the platen.

Patterned Cu wafers were employed for experiments to verify the capability of the sensor and to determine the detection schemes. A detailed layout of the pattern is shown in Fig. 3. This

pattern is transferred into a 1.5 μm thick TEOS coating with trenches etched to a depth of 1 μm on a 200 mm silicon substrate. A 20 nm Ta layer followed by a 1 μm thick PVD Cu layer was deposited on the top of the patterned oxide surface. Table 2 lists the experimental conditions.

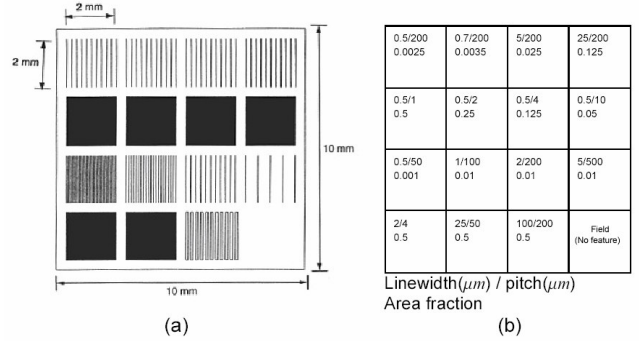


Fig. 3. Mask pattern for Cu CMP

TABLE 2
EXPERIMENTAL CONDITIONS

Experimental Parameters	Experimental Conditions
Diameter of Wafer (mm)	200
Normal Load (N)	391
Normal Pressure (kPa)	48
Rotational Speed (rpm)	75
Linear Velocity (m/s)	0.70
Duration (min)	1 - 6
Sliding Distance (m)	42 - 252
Slurry Flow Rate (ml/min)	150
Abrasive	$\alpha\text{-Al}_2\text{O}_3$
Abrasive Size (nm)	300
pH	7

IV. RESULTS AND DISCUSSION

A. Off-Line Measurements on Blanket and Patterned Wafers

Fig. 5 and Fig. 6 show the effects of surface topography on reflectance. These data were obtained off-line on patterns at the center die with various linewidths between 0.5 and 100 μm and constant Cu area fractions of 0.5. The normalized reflectance is defined as the ratio of the measured reflectance on each sub-die to the reflectance of the unpolished blanket Cu surface. By six minutes, most of the high features were removed and the surface was planarized. The smaller the pitch, the more light scatters on the surface and reduces reflectance. This can be explained by the less reflective Cu surfaces on low features due to the roughness from the deposition process. After two minutes of polishing, the normalized reflectance decreased about 0.1. The reflectance of each pattern increased gradually after the initial drop and then finally reached a steady value due to the planarization of high features.

Oxide erosion occurred after the onset of oxide exposure. The reflectance kept decreasing until all the excess Cu and barrier materials were removed. After the end-point, the reflectance remained constant, regardless of the slight nonuniformity of topography due to dishing of the soft Cu lines and rounding and erosion of the adjacent oxide regions. This again agrees with the earlier results in that the employed sensing

technique is insensitive to the small variation of the step-height. Hence, the variation of the reflectance in this regime was mainly due to the different area fraction of Cu interconnects. The areas with higher Cu area fraction are more reflective. However, the experimental values were lower than the theoretical prediction of reflectance for all patterns, especially for those with high area fractions as shown in Fig. 6.

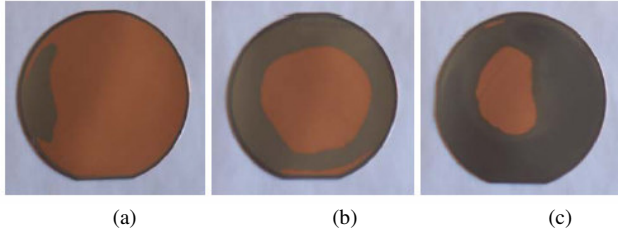


Fig. 4. Photos of blanket wafer polishing at (a) $t=2\text{min}$, (b) $t=3\text{min}$ and (c) $t=4\text{min}$

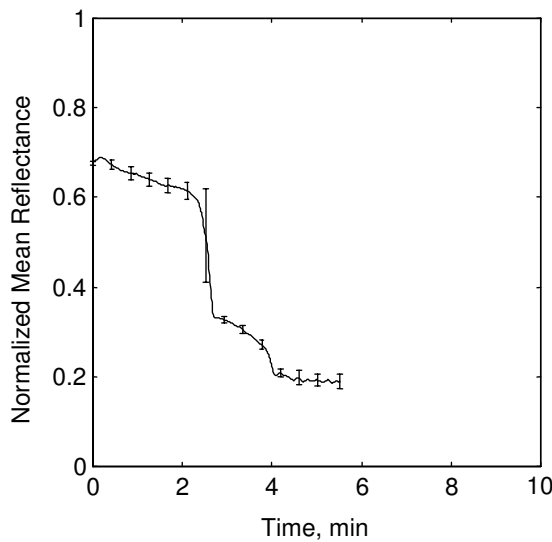


Fig. 5. Evolution of surface reflectance for the blanket wafer polishing.

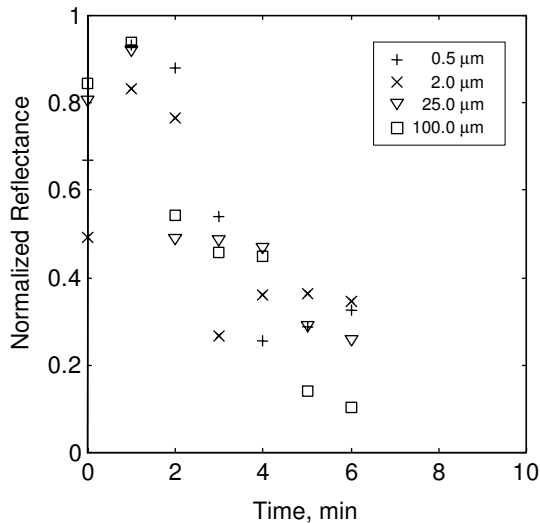


Fig. 6. The results of off-line measurements at various process regimes on the pattern with 0.5 area fraction.

B. In Situ Measurements on Patterned Wafers

Fig. 7 shows the time evolution of wafer-level reflectance data distribution and Fig. 8 shows its histogram distribution. The maximum reflectance occurred in the middle of Cu clearing regime, at about 200 seconds of polishing in this case. The low end of reflectance distribution, between 0.8 to 1.0, indicates the presence of oxide layer. As polishing time increases, this lower reflectance region expands, which represents the sub-die area on which the oxide is exposed and the peak of histogram moves to the lower limit.

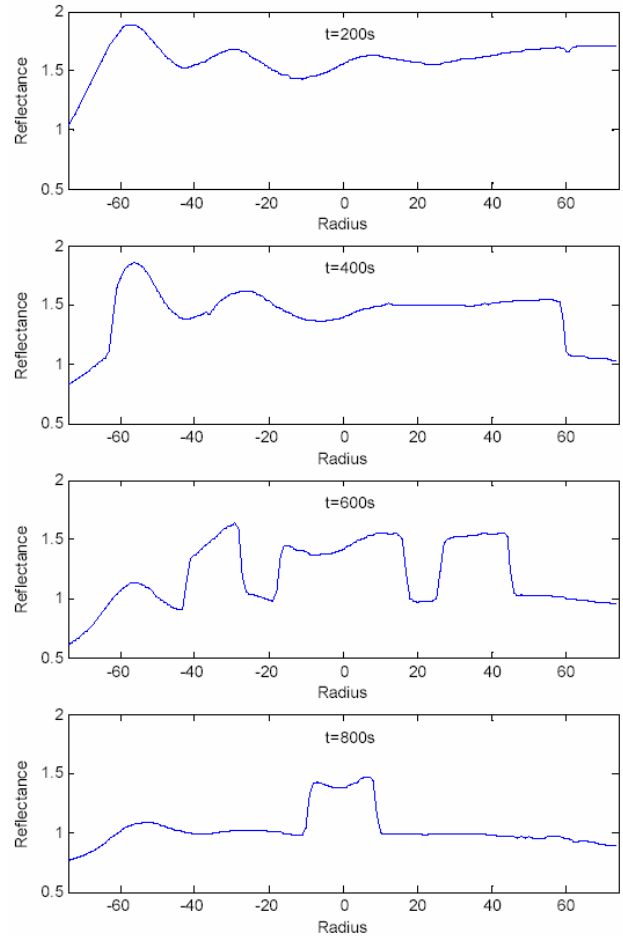


Fig. 7. Time evolution of reflectance signal for patterned wafer

Fig. 9 is an example of *in situ* measurement on a patterned Cu wafer. Because the Cu was removed nonuniformly due to the initial pattern layout and the variation of the coating thickness, the underlying oxide was gradually exposed on the surface. The mean dropped less steeply compared with data on a specific die, such as the center die. The onset of wafer-level end-point was about seven minutes in this experiment. The mean kept decreasing, but at a slower rate, after the end-point with the gradual increase of surface roughness due to overpolishing and dishing. Due to the effect of slurry and the variation of wafer-to-wafer uniformity, the mean at the onset of end-point varies in each run. Besides, the mean does not drop rapidly at the onset of end-point because the Cu is removed nonuniformly in different sub-dies and not all the dies reach the end-point at the same time. A clear sign of change in mean is lacked for

end-point indication. The mean serves only as a rough indication of the onset of process end-point.

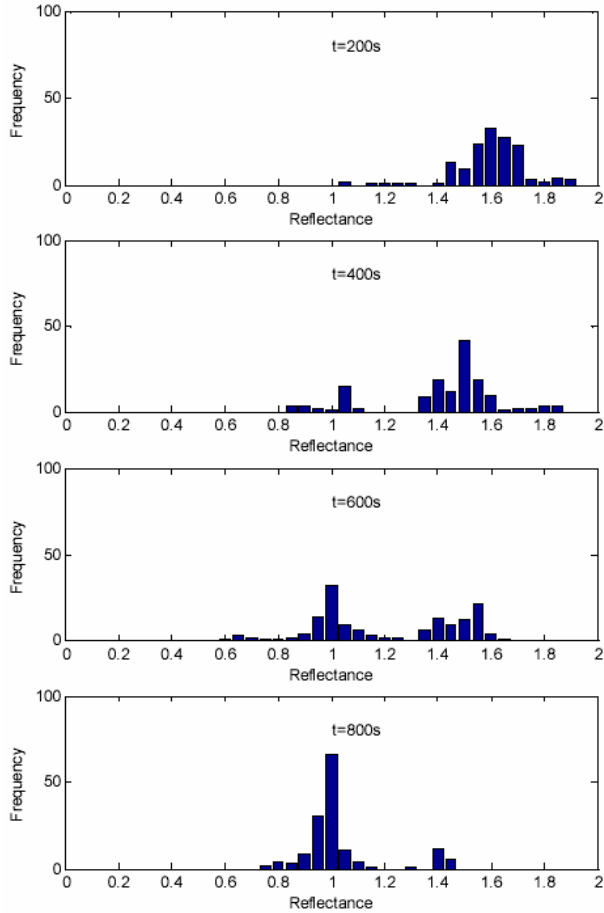


Fig. 8. Histogram of reflectance signal for patterned wafer polishing.

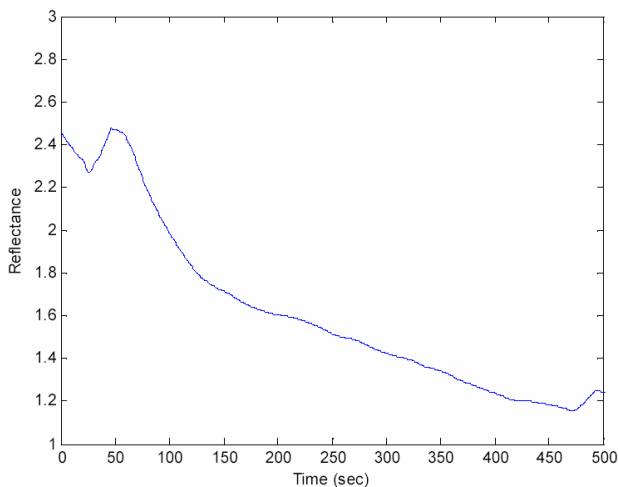


Fig. 9. Results in-situ measurements of the moving average of wafer-level surface reflectance.

Fig. 10 plots the standard deviation of the pooled data in the moving sampling set and its wafer-level and die-level components based on the nested variance analysis. Because the variation of the reflectance is mostly due to the pattern geometry and Cu area fraction, the distribution is generally not normal. The initial shape of the distribution represents the initial surface

topography of the wafer. Ideally, there are two peaks of the standard deviation during polishing. The first peak occurs at the beginning of the process corresponding to the minimum mean reflectance in the Cu planarization regime. This results from the initial surface topography and surface roughening. The standard deviation in the planarization regime reached a minimum when the majority of the pattern has been smoothed down and the mean reaches a maximum. The surface condition at this stage is similar to that of a blanket wafer. The variation of the surface reflectance is affected by the surface roughness, slurry scattering, and random error of measurement.

But in the patterned wafer, this standard variation analysis does not agree well with the actual data as shown in Fig. 10. This is mainly because the reflectance value is also dependent on the pattern geometry and its variation is not negligible.

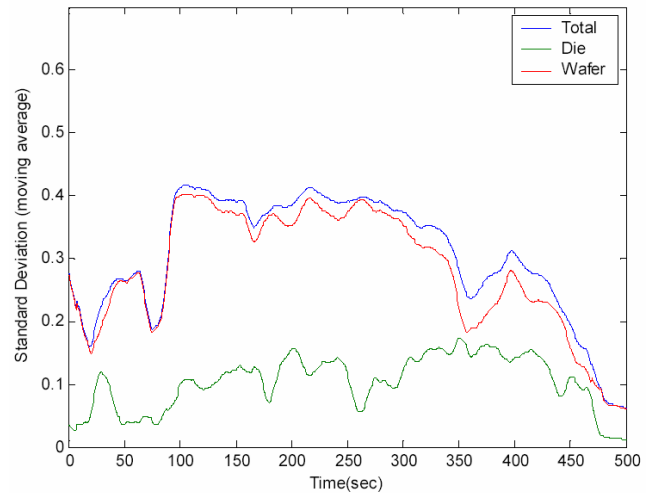


Fig. 10. Results of in-situ measurements of the standard deviation of wafer-level surface reflectance and its components at wafer-level and die-level.

The results of decomposition of estimated variance components, S_W^2 and S_D^2 with respect to the *in situ* measured data are also plotted in Fig. 10. Fig. 11 shows the value of each F ratio, defined as S_W^2 / S_D^2 , for every wafer path to examine the significance of within-wafer nonuniformity on the variation of surface reflectance. Additionally, the polishing results for all dies at the same radius are assumed to be similar and are combined into a subset for estimation of the die-level variation. The high F ratio on the wafer before polishing indicates that the within-die means at different radii are different. This is due to the variation of initial step-height from the deposition process. The within-wafer nonuniformity decreases after polishing starts, and remains at a low level with respect to the total variation. This suggests that the surface is planarized uniformly or topography becomes more uniform across the wafer through the CMP process. The within-wafer variance and the F ratio even drop to very low levels after the wafer-level end-point is reached. This is because the underlying oxide surface is harder than Cu and can retain the surface planarity and the wafer-level polishing uniformity. On the other hand, the within-die effect contributes significantly to the total variance of surface reflectance.

tance throughout the process. The process end-point can be determined based on the change of within-die variance component as a result of the drastic change of Cu area fraction. In practice, the total variance might be employed to approximate the within-die variance to determine the process end-point. The small effect of within-wafer nonuniformity will not affect the accuracy of detection.

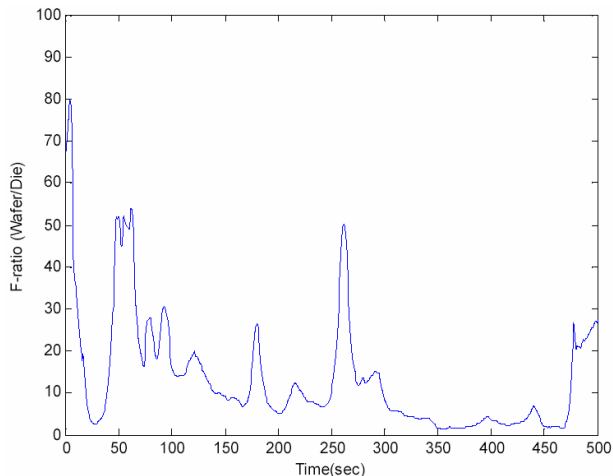


Fig. 11. Calculation of F-ratio between wafer-level and die-level variances during the polishing.

Moreover, within-wafer variance is just an indication of the nonuniform reflectance of the surface. It may not directly correlate with the uniformity of the remaining Cu thickness. However, it directly represents the uniformity of surface condition. This information can be used to monitor the across-wafer surface condition and uniformity. It may also be employed in a feedback control loop to adjust the process parameters, such as pressure distribution and velocities of wafer carrier and platen, to improve the uniformity of polishing.

Last index for detecting end-point is the Non-Uniformity, which is defined as the ratio between the standard deviation and mean of reflectance value. Fig. 12 shows NU changes as time increases. Distribution of NU is almost close to the standard deviation distribution in Fig. 10 but this can indicate the end-point better because NU value shows more flatten data.

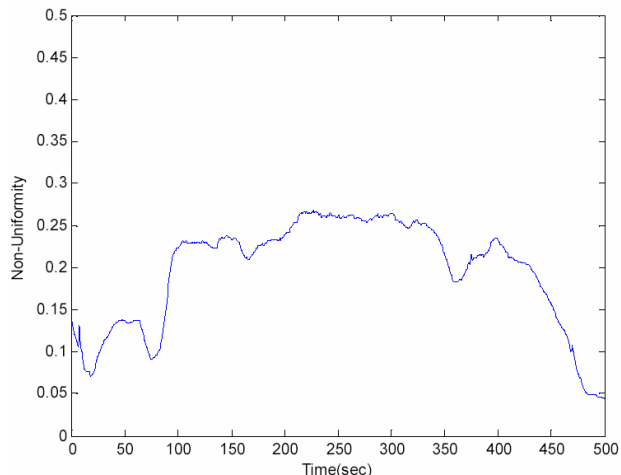


Fig. 12. Results of Non-Uniformity calculation during the polishing.

V. CONCLUSION

A statistical analysis for *in situ* reflectance sensing technique in the Cu CMP process was developed. Experiments on the patterned Cu wafers studied the effects of light scattering result due to surface roughness and the slurry particles on surface reflectance. A better decision for determining the end-point could be made based on the understanding of these systematic sources of variation.

The kinematics of the sensor was studied and its loci on the wafer were designed to cover the desired sampling area. Based on mapping the reflectance onto the wafers, a more local means of detecting the surface condition in polishing was developed. Compared with other global detection techniques, this method provides better spatial resolution and reliability in detecting the end-point. Additionally, information regarding the within-wafer nonuniform polishing was determined based on localized measurements and statistical analyses. This information may serve as feedback to control process parameters in real time to improve polishing uniformity.

Moreover, metrics for detecting process end-point, such as the mean, the variation, the range and the distribution of the surface reflectance, were developed and their effectiveness examined by experiments. The ratio σ/μ , the standard deviation divided by the mean reflectance, can effectively determine both the global and the local end-points. The ratio reaches a minimum when the end-point is achieved no matter what the pattern design is. The characteristics of various schemes with respect to different stages of polishing were also discussed. These will provide additional information for process monitoring and control for improving the quality and performance of the Cu CMP process.

REFERENCES

- [1] Banet, M.J., Fuchs, M., Rogers, J.A., Reinold, J.H., Knecht, J.M., Rothschild, M., Logan, R., Maznev, A.A., and Nelson, K.A., 1998, "High-Precision Film Thickness Determination Using a Laser-Based Ultrasonic Technique," *Appl. Phys. Lett.*, Vol. 73, pp. 169-171.
- [2] Bibby, T. and Holland, K., 1998, "End-point Detection in CMP," *J. Electronic Materials*, Vol. 27, pp. 1073-1081.
- [3] Drain, D., 1997, *Statistical Methods for Industrial Process Control*, Chapman and Hall, New York.
- [4] Litvak, H.E. and Tzeng, H.-M., 1996, "Implementing Real-Time End-point Control in CMP," *Semiconductor International*, Vol. 19, pp. 259-264.
- [5] Montgomery, D.C., 1996, *Introduction to Statistical Quality Control*, 3rd ed., John Wiley & Sons., Inc., New York, pp. 101-111.
- [6] Murarka, S., Gutmann, R., Duquette, D., and Steigerwald, J, U.S. Patent #5,637,185, June 10, 1997.
- [7] Park, T., Tugbawa, T., Boning, D., Chung, J., Hymes., 1999, "Electrical Characterization of Copper Chemical Mechanical Polishing," *Proc. 1999 CMP-MIC Conf.*, pp. 184-191.
- [8] Smith, W.L., Kruse, K., Holland, K., and Harwood, R., 1996, "Film Thickness Measurements for Chemical Mechanical Planarization," *Solid State Technology.*, Vol. 39, pp. 77-86.
- [9] Stine, B.E., 1997, "A General Methodology for Accessing and Characterizing Variation in Semiconductor Manufacturing", Ph.D. Thesis, Massachusetts Institute of Technology.
- [10] Zeidler, D., Plotner, M., and Drescher, K., 2000, "End-point Detection Method for CMP of Copper," *Microelectronic Engineering*, Vol. 50, pp. 411-416.